

Supplementary: Functional connectivity of fMRI using differential covariance predicts structural connectivity and behavioral reaction times

Yusi Chen, Qasim Bukhari, Tiger W. Lin, Terrence Sejnowski

| Variable | Annotation | HCP (B=3T) | Mouse (B=9.4T) |
|---------------|---------------------------------------------------------------------------------------------|---------------|-------------------|
| ϑ_0 | Frequency offset at the outer surface of the magnetized vessel for fully deoxygenated blood | 80.6 [2] | 252.5 [2] |
| ρ | Oxygen extraction fraction | 0.8 | 0.8 |
| ϵ | Ratio of intra- and extravascular signal | 0.5 | 0.5 |
| r_0 | Slope of the relation between intravascular relaxation rate and oxygen saturation | 167 [4] | 458 [1] |
| TE | Time of echo (ms) | 30 | 40 |
| τ | haemodynamic transit time | 0.98 | 0.98 |
| α | Grubbs exponent | 0.32 | 0.32 |
| κ | Rate of signal decay | 0.65 | 0.65 |
| γ | Rate of flow-dependent elimination | 0.41 | 0.41 |
| η | Neuronal efficacy | 0.54 | 0.54 |
| V_0 | Resting blood volumne fraction | 0.02 | 0.02 |

Table S1: Parameters used in backward reconstruction

Table S2: **Annotated components for HCP dataset.** First column is the index number of pre-selected IC components. Second column is the manually registered anatomical region. Third column is the assigned sub-network. DMN: default mode network

| Component number | Anatomical Region | Sub-network |
|------------------|----------------------------------------------------------------------------------------|----------------------|
| 1 | Occipital Pole | Visual Network |
| 2 | Inferior Parietal Lobe | DMN |
| 3 | Lateral Occipital Cortex | Visual Network |
| 4 | Cuneal Cortex/Occipital Pole | Visual Network |
| 5 | Supramarginal Gyrus | DMN |
| 6 | Lateral Occipital Cortex | Visual Network |
| 7 | Supramarginal Gyrus | DMN |
| 8 | Lateral Occipital Cortex | Visual Network |
| 9 | Inferior Parietal Lobe | DMN |
| 10 | Medial Prefrontal Cortex/Anterior Cingulate Cortex/Lateral Temporal Cortex | DMN |
| 11 | Lingual Gyrus/medial occipitotemporal gyrus | Visual Network |
| 12 | Angular Gyrus | DMN |
| 13 | Occipital Pole | Visual Network |
| 14 | Lateral Occipital Cortex - Left | Visual Network |
| 15 | Precuneous Cortex | Other Network |
| 16 | Occipital Pole | Visual Network |
| 17 | Lingual Gyrus/medial occipitotemporal gyrus | Visual Network |
| 18 | Lateral Occipital Cortex | Visual Network |
| 19 | Occipital Pole | Visual Network |
| 20 | Inferior Parietal Lobe | DMN |
| 21 | Precentral Gyrus | sensorimotor network |
| 22 | Orbital Frontal Cortex | DMN |
| 23 | Postcentral Gyrus | sensorimotor network |
| 24 | Lateral Occipital Cortex - Right | Visual Network |
| 25 | Occipital Pole - Left | Visual Network |
| 26 | Frontal Pole | Attention Network |
| 27 | Superior Parietal Lobule | Attention Network |
| 28 | Hippocampus/Parahippocampal Cortex | DMN |
| 29 | Lateral Temporal Cortex | DMN |
| 30 | Lateral Occipital Cortex | Visual Network |
| 31 | Orbital Frontal Cortex/Lateral Temporal Cortex | Other Network |
| 32 | Occipital Pole | Visual Network |
| 33 | Inferior Parietal Lobe – Left | DMN |
| 34 | Lateral Occipital Cortex | Visual Network |
| 35 | Postcentral Gyrus | sensorimotor network |
| 36 | Medial Prefrontal Cortex/Anterior Cingulate Cortex | DMN |
| 37 | Orbital Frontal Cortex/Lateral Temporal Cortex | DMN |
| 38 | Precentral Gyrus / Juxtapositional Lobule Cortex (formerly Supplementary Motor Cortex) | sensorimotor network |
| 39 | Occipital Pole | Visual Network |
| 40 | Middle Frontal Gyrus | Attention Network |
| 41 | Postcentral Gyrus - Left | sensorimotor network |
| 43 | Postcentral Gyrus - Right | sensorimotor network |
| 44 | Orbital Frontal Cortex | DMN |
| 45 | Superior Temporal Gyrus | sensorimotor network |
| 48 | Frontal Pole | Attention Network |
| 49 | Lateral Occipital Cortex | Visual Network |
| 50 | Occipital Fusiform Gyrus | Visual Network |
| 60 | Hippocampus/Parahippocampal Cortex | DMN |
| 64 | Hippocampus/Parahippocampal Cortex | DMN |
| 67 | Thalamus | Thalamic Network |
| 69 | Putamen | sensorimotor network |
| 76 | Putamen - Right | sensorimotor network |
| 78 | Right V1 | Visual Network |
| 82 | Left V1 | Visual Network |
| 84 | Visual Cortex | Visual Network |
| 87 | Thalamus | Thalamic Network |
| 92 | Right V1 | Visual Network |
| 93 | Left V1 | Visual Network |
| 96 | Thalamus - Right | Thalamic Network |
| 97 | Thalamus - Left | Thalamic Network |

Table S3: Annotated IC maps for the Bukhari mouse dataset. First column is the index of pre-selected IC components. Second column is the manually registered anatomical region. Third column is the corresponding anatomical locations in the Swanson database [3]. SSp = Primary somatosensory area , SSs = Supplemental somatosensory area, MO = Somatomotor areas, ACAd(v) = Anterior cingulate area dorsal (ventral), RSPd(v) = Retrosplenial region dorsal (ventral), CEA = Central amygdalar nucleus, MEA = Medial amygdalar nucleus, AAA = Anterior amygdalar area, BMA = Basomedial amygdalar nucleus, PAA = Piriform-amamygdalar area, IA = Intercalated amygdalar nuclei, AAA = Anterior amygdalar area, BLA = Basolateral amygdalar nucleus, LA = Lateral amygdalar nucleus, PA = Posterior amygdalar nucleus, ECT = Ectorhinal area, PERI = Perirhinal area, CP = Caudoputamen, AI = Agranular insular, PIR = Piriform area, GP = Globus pallidus, NA: no corresponding anatomical locations in the database

| IC number | Full Name | Swanson region (Abbreviations) | Subnetwork |
|-----------|------------------------------------------|--------------------------------------|------------------------------|
| 1 | Primary Somatosensory Cortex (both side) | SSp | Lateral cortical network |
| 2 | Secondary Sematosensory Cortex (right) | SSs | Lateral cortical network |
| 3 | Secondary Sematosensory Cortex (left) | SSs | Lateral cortical network |
| 4 | Primary Somatosensory Cortex (right) | SSp | Lateral cortical network |
| 5 | Primary Somatosensory Cortex (left) | SSp | Lateral cortical network |
| 6 | Motor Cortex (right) | MO | Lateral cortical network |
| 7 | Motor Cortex (left) | MO | Lateral cortical network |
| 8 | Anterior Cingulate Cortex, dorsal | ACAd | Default mode network |
| 9 | Cingulate Cortex/ Retrosplenial Cortex | ACAv/ACAd/RSPd/RSPv | Default mode network |
| 10 | Amygdalar (right) | CEA/MEA/AAA/BMA/PAA/IA/AAA/BLA/LA/PA | Associative cortical network |
| 11 | Amygdalar (left) | CEA/MEA/AAA/BMA/PAA/IA/AAA/BLA/LA/PA | Associative cortical network |
| 12 | Ectorhinal Cortex (left) | ECT | Associative cortical network |
| 13 | Ectorhinal Cortex (right) | ECT | Associative cortical network |
| 14 | Perirhinal Area (right) | PERI | Associative cortical network |
| 15 | Caudoputamen (right) | CP | Subcortical network |
| 16 | Caudoputamen (left) | CP | Subcortical network |
| 17 | Insular (left) | AI | Associative cortical network |
| 18 | Insular (right) | AI | Associative cortical network |
| 19 | Insular (left) | AI | Associative cortical network |
| 20 | Insular (right) | AI | Associative cortical network |
| 21 | Perirhinal Area (right) | PERI | Associative cortical network |
| 22 | Perirhinal Area (left) | PERI | Associative cortical network |
| 23 | Piriform Cortex (left) | PIR | Associative cortical network |
| 24 | Piriform Cortex (right) | PIR | Associative cortical network |
| 25 | Globus Pallidus (right) | GP | Subcortical network |
| 26 | Globus Pallidus (left) | GP | Subcortical network |
| 27 | Thalamus, dorsal (left) | NA | Thalamic network |
| 28 | Thalamus, dorsal (right) | NA | Thalamic network |
| 29 | Thalamus, ventral (left) | NA | Thalamic network |
| 30 | Thalamus, ventral (right) | NA | Thalamic network |

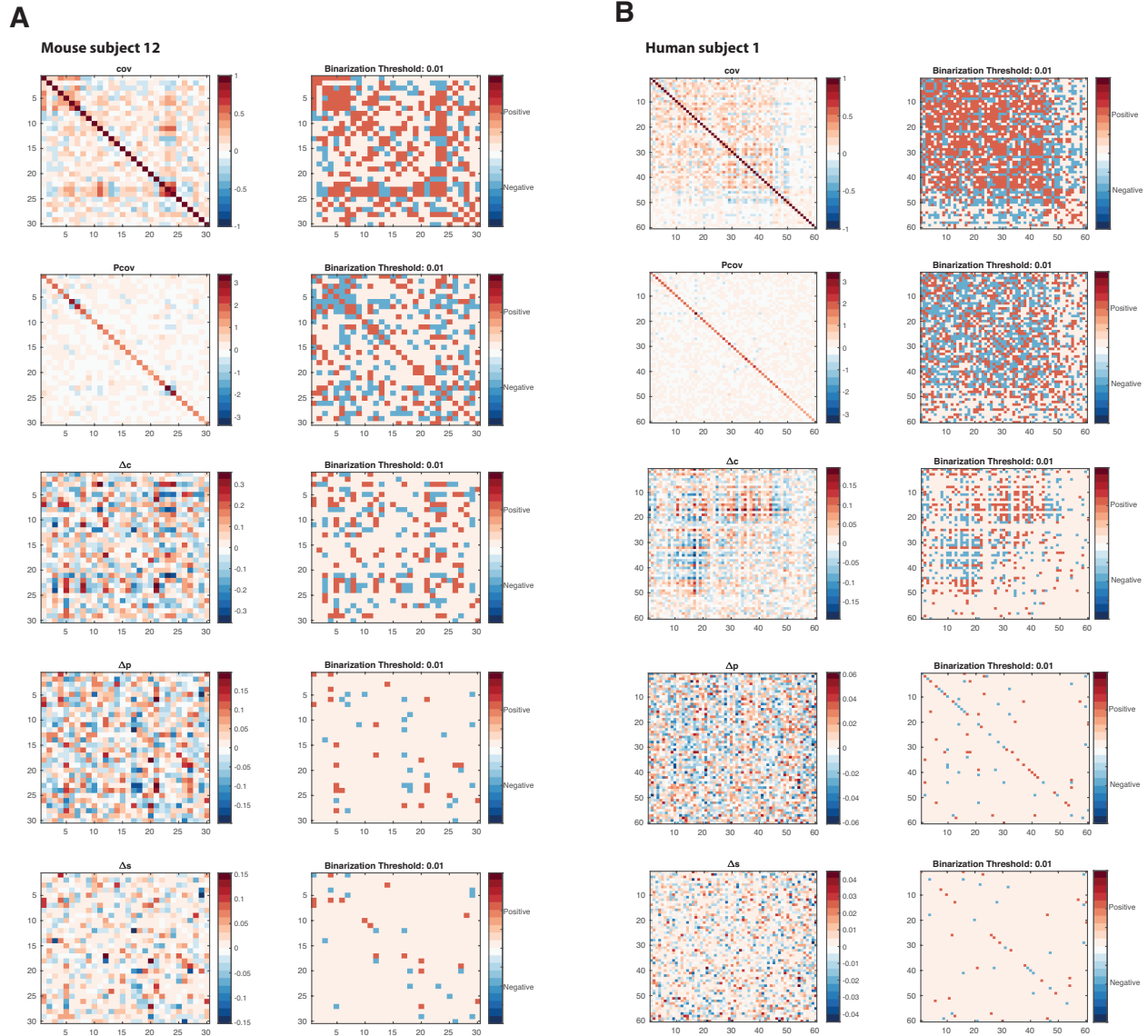


Figure S1: Differential covariance based methods produce sparse and directed FC. Example covariance matrix (cov), precision matrix (Pcov), Δc , Δp and Δs and their binarized matrices (right) of one mouse subject (A) and one human subject (B).

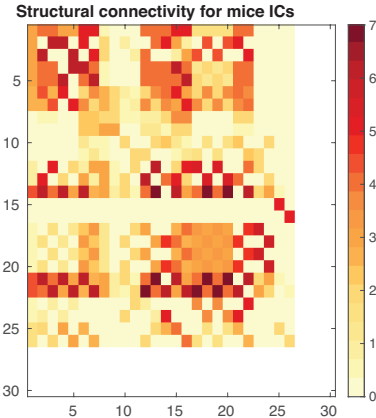


Figure S2: The structural connectivity matrix for mouse

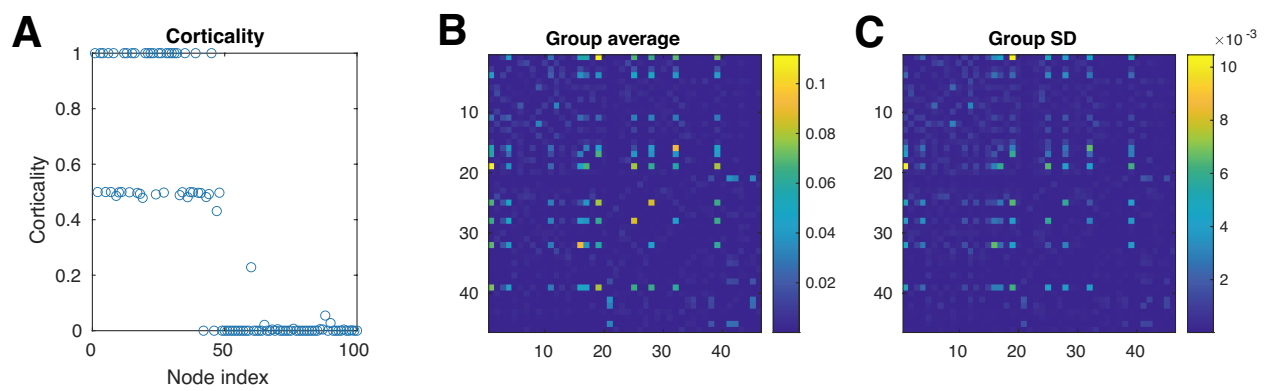
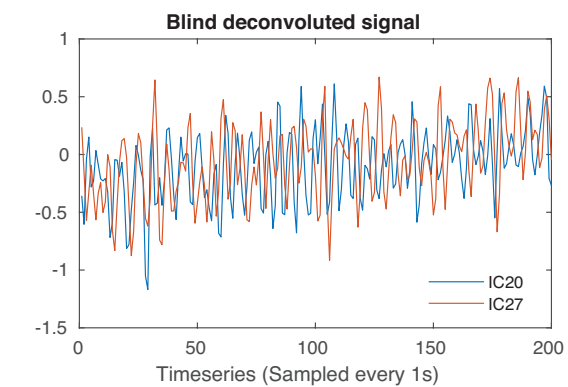
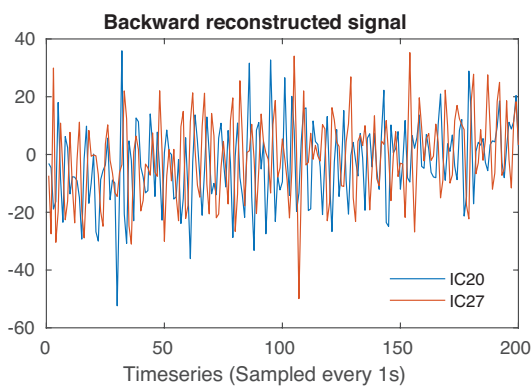
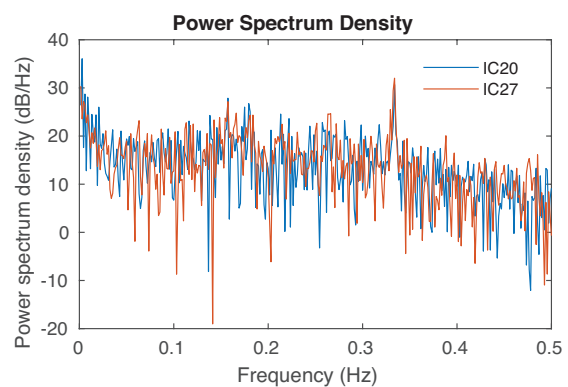
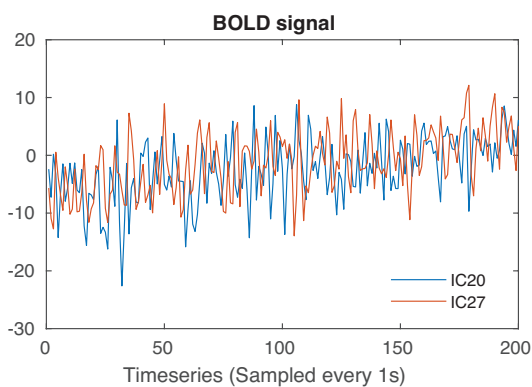


Figure S3: Individual level dMRI statistics. (A) Corticity was defined as the proportion of cortical voxels within each IC. Since dMRI measurements are only available for cortical surface voxels. Our analysis was restricted to the first 46 ICs with corticity greater than 40%. (B) Average of the dMRI matrices across the entire 998 subjects. (C) Standard deviation.

A

Mouse subject 2, time traces of IC20 and IC27

**B**

Human subject, time traces of IC45 and IC48

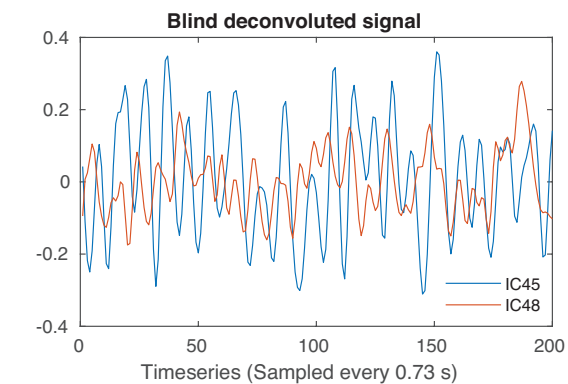
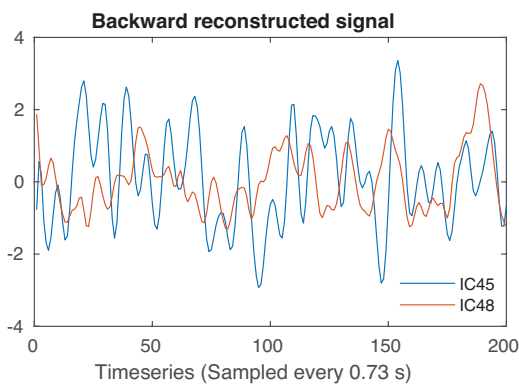
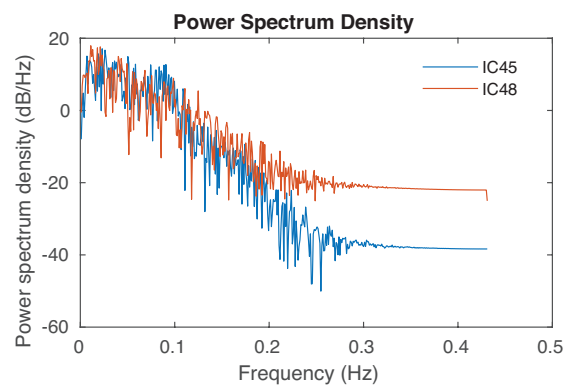
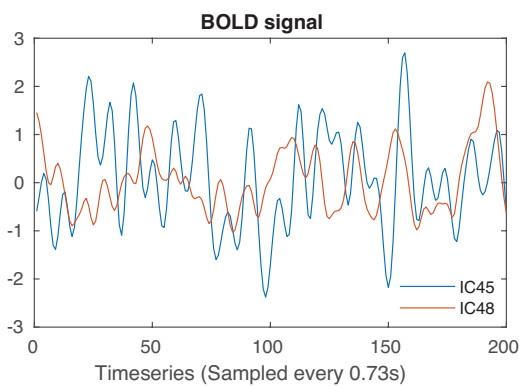


Figure S4: Two example time traces from one mouse subject (A) and one human subject (B)
 Upper left: haemodynamic signal after dual regression; Upper right: power spectrum density of the haemodynamic signal; Lower left: backward reconstructed signal; Lower right: blind deconvoluted signal

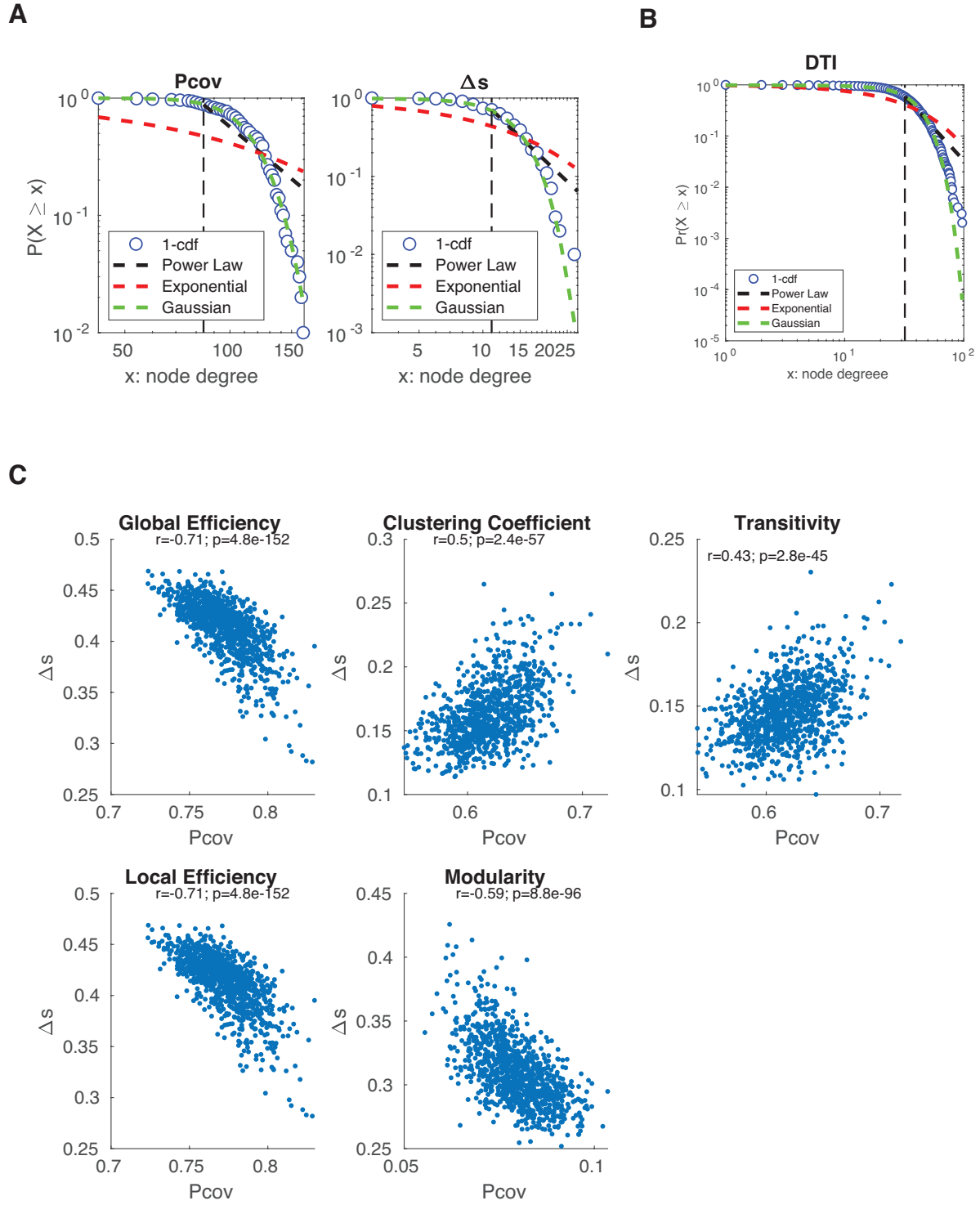


Figure S5: Network topology analysis of FC. (A) Cumulative density function of network degree distribution of Pcov-FC and Δs -FC from one HCP subject. (B) Network degree distribution of structural connectivity matrix from diffusion tensor imaging (DTI). (C) Scatterplots of global efficiency, local efficiency, clustering coefficient, transitivity and modularity of Δs -FC versus that of Pcov-FC.

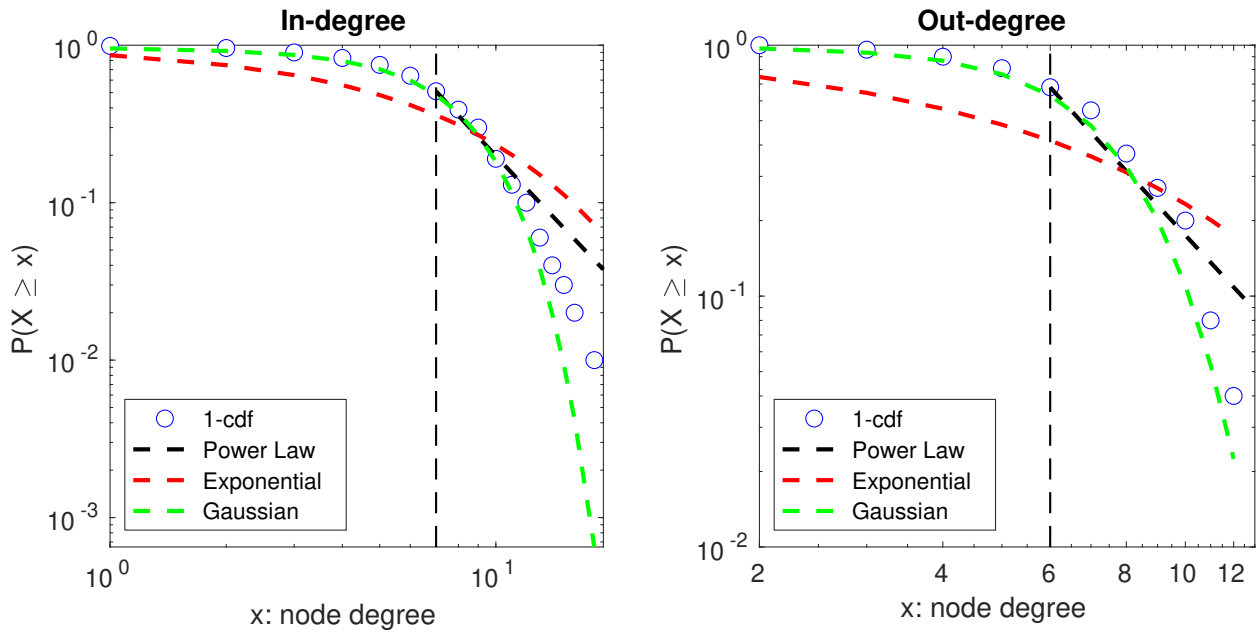


Figure S6: In-/Out- degree node distribution for Δ_s -FC

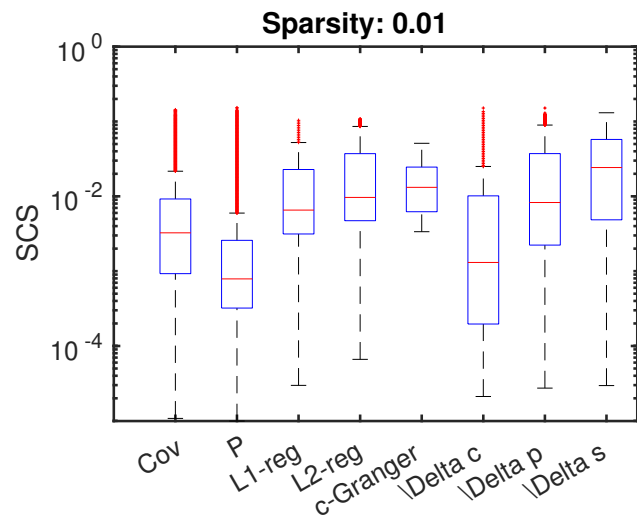


Figure S7: SCS of all subjects inferred from different methods thresholded to a same sparsity level. Δ_s still have significantly higher (ranksum test, $p < 10^{-34}$) SCS values compared to all other methods. \Delta stands for Δ

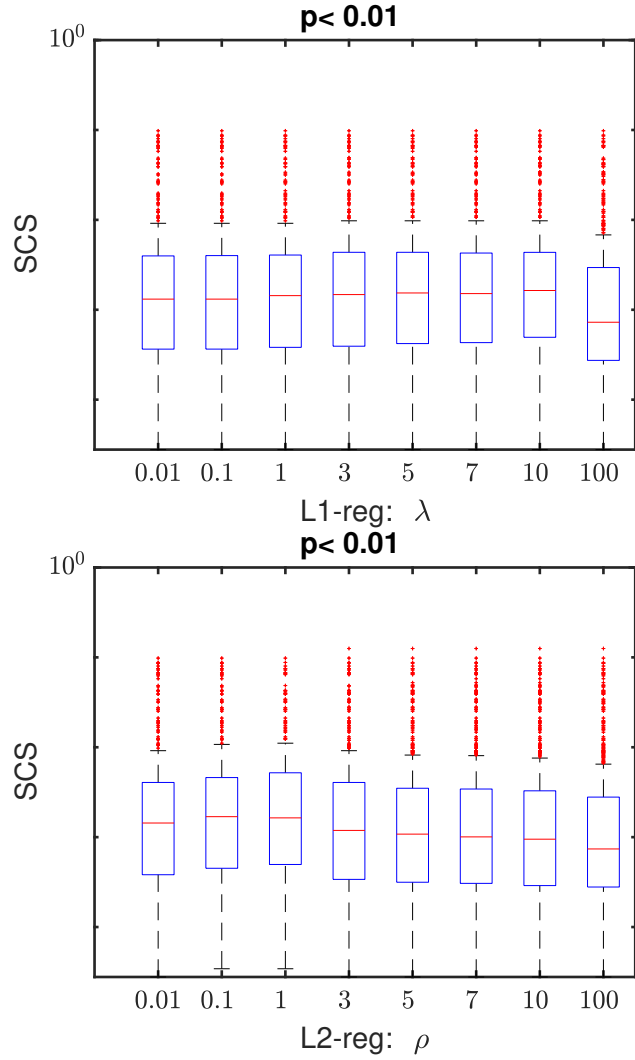


Figure S8: SCS of one HCP subject inferred by L1-/L2-reg penalized to different extents (λ and ρ). The default value used in the main text is $\lambda = 10$ and $\rho = 0.1$. All other parameters showed similar (no statistical difference) or worse performance. The binarization threshold was $p < 0.01$.

References

- [1] Sang-Pil Lee, Afonso C Silva, Kamil Ugurbil, and Seong-Gi Kim. Diffusion-weighted spin-echo fmri at 9.4 t: microvascular/tissue contribution to bold signal changes. *Magnetic Resonance in Medicine: An Official Journal of the International Society for Magnetic Resonance in Medicine*, 42(5):919–928, 1999.
- [2] S Ogawa, RS Menon, David W Tank, SG Kim, H Merkle, JM Ellermann, and K Ugurbil. Functional brain mapping by blood oxygenation level-dependent contrast magnetic resonance imaging. a comparison of signal characteristics with a biophysical model. *Biophysical journal*, 64(3):803–812, 1993.
- [3] Larry W Swanson, Joel D Hahn, Lucas GS Jeub, Santo Fortunato, and Olaf Sporns. Subsystem organization of axonal connections within and between the right and left cerebral cortex and cerebral nuclei (endbrain). *Proceedings of the National Academy of Sciences*, 115(29):E6910–E6919, 2018.
- [4] Jason M Zhao, Chekesha S Clingman, M Johanna Närväinen, Risto A Kauppinen, and Peter CM van Zijl. Oxygenation and hematocrit dependence of transverse relaxation rates of blood at 3t. *Magnetic Resonance in Medicine: An Official Journal of the International Society for Magnetic Resonance in Medicine*, 58(3):592–597, 2007.